PHILOSOPHICAL TRANSACTIONS OF THE ROYAL SOCIETY A MATHEMATICAL, PHYSICAL & ENGINEERING SCIENCES

All-Optical Logic in Optical Waveguides

H. A. Haus and N. A. Whitaker

Phil. Trans. R. Soc. Lond. A 1984 **313**, 311-319
doi: 10.1098/rsta.1984.0112

Phil. Trans. R. Soc. Lond. A **313**, 311–319 (1984)
Printed in Great Britain

All-optical logic in optical waveguides

By H. A. Haus and N. A. Whitaker, Jr

Department of Electrical Engineering and Computer Science and Research Laboratory of Electronics, Massachusetts Institute of Technology, Cambridge, Massachusetts 02139, *U.S.A.*

The motivation for the development of all-optical logic elements in integrated optical waveguides is reviewed. The difficulties inherent in the 'all-optical' approach are outlined. The all-optical, universal logic for pipeline operation based on the Mach–Zehnder interferometer is described and experiments on a prototype all-optical modulator fabricated in $LiNbO_3$ are presented. The paper concludes with a discussion of a device design for operation with shorter lengths and compatible with semiconductor laser drives.

1. Introduction

The advances made in the last few years in reducing the loss and increasing the bandwidth of optical fibres are unprecedented. According to the latest reports, a fibre link 161.5 km in length was operated at 420 Mbit s^{-1} at a wavelength of 1.55 μm (Kasper *et al.* 1983). Shorter fibre links could accommodate higher bit rates, and further progress will no doubt be made in reducing the dispersion in all-optical fibres. The stage is set for optical communication links whose bit rates are enormous compared with contemporary usage. Thus far, however, the optical signals are detected, processed and recorded electronically, not optically.

All-optical signal-processing devices will compete successfully with the current electronic devices by offering unique processing capabilities. Some of these capabilities are listed below.

(*a*) For signals that are already optical, an all-optical signal-processing stage has a natural advantage, provided that it is not of much greater complexity than its electronic counterpart.

(*b*) The absolute bandwidths that are achievable in optical circuits are much larger than those of electronic circuits. It is not an accident that the shortest pulses measured (Fujimoto *et al.* 1984) are optical, not electronic.

(*c*) The introduction of single-mode fibres has advanced the fabrication technology of optical waveguide signal-processing devices because such devices are compatible only with single-mode fibres, not with their more common multimode counterpart.

The circumstances cited above give all-optical, single-mode waveguide signal-processing devices a competitive edge over their electronic counterparts. We are not addressing here two-dimensional signal-processing devices which by their two-dimensionality offer certain unique characteristics. It is well to keep in mind that the handicaps of all-optical single-mode waveguide devices are severe in the race against their electronic competitors, as shown below.

(i) Optical waveguides have large dimensions. Their cross-sectional widths are at least several wavelengths and their interaction lengths are often of the order of millimetres. This must be compared with a microwave FET of 1 μm 'length' and submillimetre 'widths'.

(ii) The topology of optical waveguides is cumbersome. They cannot be 'bent' as easily as a transmission line, and waveguides cannot easily be made to cross.

(iii) Electronic devices need to operate with switching energies that are large compared with kT to prevent random switching (k = Boltzmann's constant, T = thermodynamic temperature). Optical devices must have switching energies large compared with the photon energy $h\nu$ to avoid photon noise.

(iv) Optical nonlinearities are weak compared with electronic nonlinearities.

(v) Optical devices require a continuous optical input, whereas maintenance of a switching state in CMOS is achieved with virtually no supply of power.

The great single advantage offered by all-optical signal processing is its speed; if speed of response is an overriding concern, optical signal processing will always maintain a competitive edge over the electronic alternative.

In this paper we concentrate on a proposed travelling-wave all-optical waveguide device that can be adapted to operate as an AND gate, OR gate, XOR gate, or as an inverter. The device operates in the 'pipeline mode', i.e. a stream of pulses is continuously processed, interacting within a time interval τ and emerging at the output after a delay equal to the interaction time. Since the required pulse energy is proportional to $1/\tau$, lower pulse energies can be achieved by increasing τ, thereby increasing the delay. The speed of the device is solely a function of the energy relaxation time in the material, but not the interaction time. This should be contrasted with the standing-wave Fabry–Perot type devices (Gibbs *et al.* 1979), in which the interaction time also determines the response time.

In §2 we describe the operation of the device and experimental results obtained with a device fabricated in $LiNbO_3$ that performed as a picosecond all-optical waveguide modulator. Section 3 discusses a proposed version of the device that can operate, in principle, with 'multiple quantum well' (m.q.w.) structures at power levels compatible with semiconductor laser diodes. The response time of the device is sharpened (relative to the 20 ns relaxation time in a m.q.w. structure) by means of lateral carrier diffusion, as outlined in §4.

2. The all-optical Mach–Zehnder interferometer

One requirement for an all-optical logic device is that it should operate with mutually incoherent optical excitations because maintenance of phase coherence is too severe a requirement in any practical system. It is also desirable to use the same frequency for the interacting pulses. The proposed all-optical logic gate based on the Mach–Zehnder interferometer satisfies these requirements (Lattes *et al.* 1983). This device uses single-mode optical waveguides as shown in figure 1. A pulse enters the central guide in a TM mode. The two 'control' guides are excited by pulses in the TE mode. The interferometer performs different functions depending on the d.c. bias voltage applied to the electrodes.

If the field is such that the phase difference in the two arms of the interferometer is π and no pulse enters the 'control' guides, then an antisymmetric field pattern is produced at the output waveguide 'Y'. Because the output waveguide is a single-mode guide this field (which corresponds to a higher-order antisymmetric mode) is not confined to the waveguide and escapes into the substrate: no output occurs. Next consider the case when one TE pulse enters either one of the two control guides. If the intensity of the control pulse is adjusted so as to produce an index change Δn such that $(\omega/c)\,\Delta n l = \pi$, the bias π phase shift is cancelled and the TM pulse emerges at the output.

Of course the π phase shift occurs only at the peak intensity, and cancellation over the entire

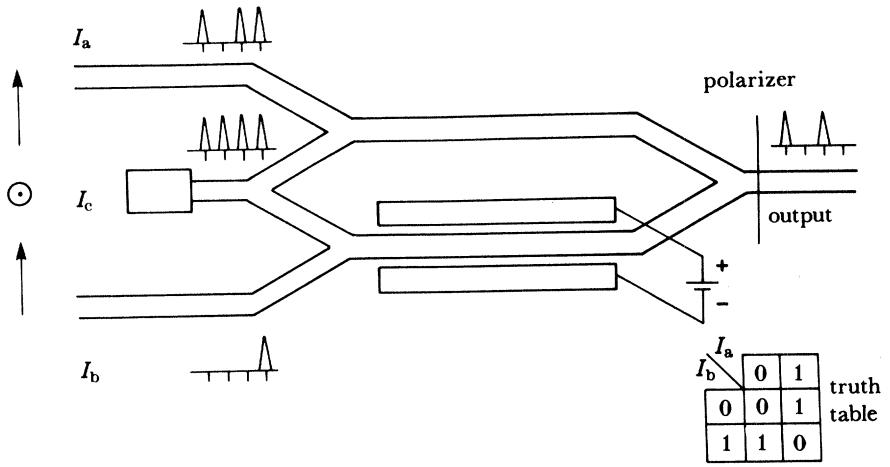

FIGURE 1. Schematic diagram of the optically modulated Mach–Zehnder waveguide interferometer.

pulse duration is not perfect, as some distortion occurs. This distortion can be overcome if there is birefringence such that the pulses 'slip' through one another, effectively broadening the time window within which the change Δn occurs as seen by the TM pulse. The device operates as an XOR gate, as indicated by the inset in figure 1. Figure 2 shows other possible functions of the interferometer, corresponding to different choices of the bias and different choices of inputs and outputs.

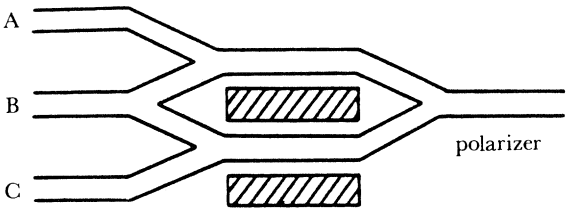

function	*inputs*	*phase shift*	*comment*
inverter	A	0	pulse stream in C
XOR	A, B	0	pulse stream in C
AND	A, C	π	no pulse stream
XOR	A, B	π	pulse stream in C

FIGURE 2. Possible functions of interferometer for different biases and different input ports.

Such a device has been fabricated in Z-cut Y-propagating $LiNbO_3$ to demonstrate some of its features (Lattes *et al.* 1983). The power required to operate an XOR gate of total interaction length $L = 2$ cm was estimated by Miller's rule to be of the order of 150 W. In fact the operation of the device was the first measurement of the coefficient $\chi^{(3)}_{xxzz}$ expressed as n_2 and found to be $n_2 = 3 \times 10^{-9}$ cm^2 MW^{-1}. This called for a drive power roughly 10 times greater than predicted. Because only about 2 W peak power was provided in the interaction region, only *modulation* of one optical pulse by the other could be demonstrated. The control pulse was shifted relative to the controlled pulse by an interferometer arrangement, as shown in figure 3. The electrode voltage was switched to give phase shifts of $-\frac{1}{2}\pi$ and $\frac{1}{2}\pi$ alternately to provide maximum positive and negative response sensitivity and the response was measured on a dual trace scope. The

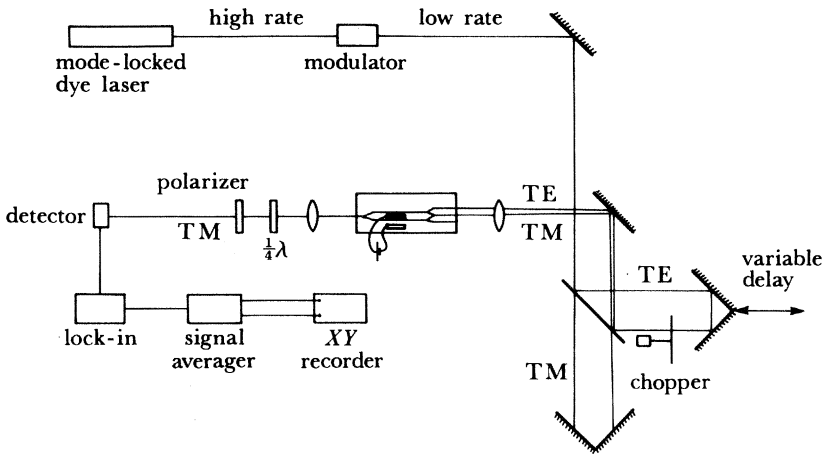

FIGURE 3. Experimental set-up for testing a modulator.

measured full-width half maximum of the pulses shown in figure 4 is 10 ps. The pulses appear to be 'extended' because the pulses slip through one another owing to the birefringence of $LiNbO_3$. Other pertinent experimental parameters are summarized in table 1.

This experiment demonstrated, in effect, the first all-optical modulator. A practical device, operated from a semiconductor laser and of shorter length, requires a material of much larger nonlinearity. The measured n_2 in GaAs is two orders of magnitude larger than the n_2 found in $LiNbO_3$ (Chen & Carter 1982).

We are currently fabricating such an interferometer in GaAs. This structure is not yet practical owing to its excessive length (1 cm) and the required peak power (20 W). The device becomes practical only if one could drastically reduce the power requirement. The very large

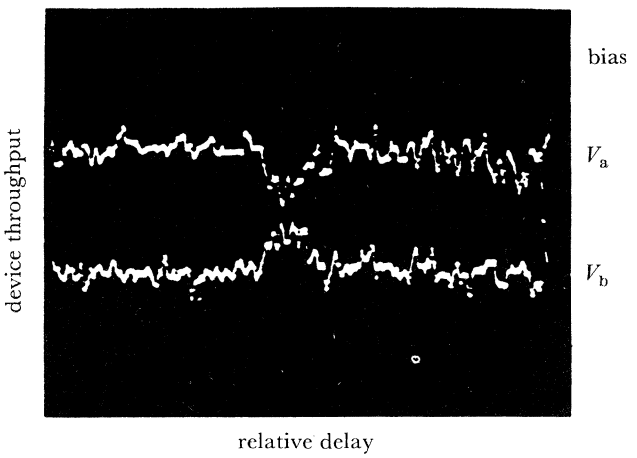

FIGURE 4. Response of modulator. The two traces are obtained by switching the bias voltage to produce $\frac{1}{2}\pi$ and $-\frac{1}{2}\pi$ phase shifts respectively and displaying the interferometer response on a dual-trace oscilloscope.

TABLE 1. EXPERIMENTAL CONDITIONS

source	synchronously pumped Kr^+ ion laser
dye	oxazine 750/pc and ethylene glycol
tuning range	720–900 nm
pulse duration	5 ps
repetition rate	80 MHz
this work	peak power, 200 W; λ, 850 nm

nonlinearities found in multiple quantum well GaAs would require a much lower drive power. The response time of room-temperature excitons in m.q.w. GaAs is of the order of 20 ns and additional modifications are therefore necessary to achieve a fast all-optical gate. In the last section we discuss some of these issues as well as a design that operates with 1 W peak power and less than 300 ps response time. Faster operation at low power levels still awaits new material developments of a new device design.

3. A waveguide interferometer with m.q.w. structure

Operation of a multiple quantum well device faster than 50 MHz (*ca.* 1/(20 ns)) requires a speeding-up of the carrier relaxation rate. Fast traps to aid carrier recombination are not appropriate because they fill up under steady-state excitation. Carrier sweepout by using either drift or diffusion are possibilities. To achieve acceptable nonlinear index changes, it is necessary to produce carrier densities greater than 10^{17} cm^{-3}. Under these conditions carrier transport can be adversely affected by ambipolar effects.

For the carrier drift not to be ambipolar (and unacceptably slow) it is necessary for the applied field not to be reduced appreciably when the positive and negative charge carriers are pulled to the opposite electrodes. For a density of $N = 10^{17}$ cm^{-3} photocarrier pairs to be swept out over a distance of $d = 1$ μm, the applied field, E, would have to be greater than eNd/ϵ, where e is the charge on the electron and ϵ the dielectric constant. This corresponds to a field of 1.4×10^6 V cm^{-1} for a relative dielectric constant of 13. This field is large compared with a field, E_d, that destroys the excitons.

This field may be estimated from $eE_d d = B$, where d is the exciton diameter and B is the two-dimensional exciton binding energy. This gives $E_d = 2 \times 10^4$ V cm^{-1}. Carrier removal by drift only can be accomplished over distances of the order of 0.1 μm. This distance is small compared with a wavelength and entails operation of the nonlinear medium in the fringing field of the optical waveguide. Whereas sweepout by drift may not be impossible, the device proposed here uses sweepout by diffusion.

Figure 5 shows a schematic diagram of such a device, designed to operate by carrier diffusion. The vertical and horizontal scales are widely different. The inset shows the cross section through the waveguide with the layered m.q.w. material. The barrier and well dimensions are chosen to be approximately 10 nm, which is a workable compromise for good exciton confinement without excessive inhomogeneous broadening (Chemla *et al.* 1984). The optical index is changed in the electro-optic tuning section by means of the applied electrodes on top of the waveguides.

The excitonic resonance is dissipative at the centre of the exciton line with a reactive part that peaks and then diminishes as one detunes from line centre. Detuning is also accompanied by a decrease of the nonlinearity, so that minimization of drive power and minimization of device throughput loss are at odds. The response I_o/I_i of the device, equal to the ratio of the output power to the input power of the controlled pulse, is controlled by a change of absorption coefficient ($\Delta\alpha$) and a phase change ($\Delta\phi$) away from the applied π phase shift in one arm. This can be easily determined from the symmetric part of the resulting mode pattern,

$$I_o/I_i = e^{-\alpha_0 L}\{\sin^2(\tfrac{1}{2}\Delta\phi)\, e^{-\frac{1}{2}\Delta\alpha L} + \tfrac{1}{4}(1 - e^{-\frac{1}{2}\Delta\alpha L})^2\}, \quad (1)$$

where α_0 is the linear (constant) loss.

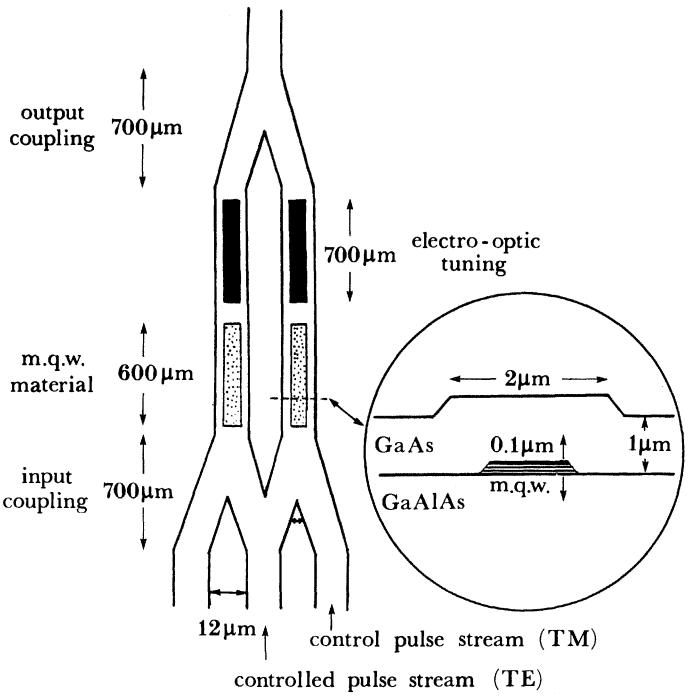

FIGURE 5. Schematic diagram of interferometer design incorporating m.q.w.

The effective phase shift, $\Delta\phi$, and loss saturation can be evaluated from the assumed simple saturation formula

$$\alpha(I) = \alpha_0/(1+I/I_s), \tag{2}$$

where

$$I_s = \hbar\omega/2L_z A_x \alpha_0 \tau_p.$$

Here L_z is the width of the quantum well, A_x is the exciton area and τ_p is the pulse length. The susceptibility has the same intensity dependence. No measurements are available of the m.q.w. absorption spectrum with the polarization perpendicular to the layers. The control mode, assumed to be polarized perpendicularly to the layers, produces carrier density changes that affect the absorption, as indicated by (2). We assume that the absorption of the control mode is given by the same formula as that of a mode polarized parallel to the layers. The controlled mode is assumed to be weaker than the control mode so that its saturation effects can be ignored.

From (2) we find that α changes according to the law

$$\Delta\alpha = \alpha_0 - \frac{\alpha_0}{1+(I/I_s)} = -\frac{\alpha_0(I/I_s)}{1+(I/I_s)}.$$

The change of index follows the same saturation law except that the proportionality constant is n_0, rather than α_0; n_0 can be related to α_0 by Kramers–Kronig relations and is a function of the frequency deviation from the heavy-hole exciton absorption-line centre. The intensity decays with distance due to the absorption saturation of photons and the creation of

charged-carrier pairs. Ignoring the absorption saturation ($I(x) \approx I_i e^{-\alpha_0 x}$), $\Delta\phi$ is obtained from the integral

$$\Delta\phi = \frac{2\pi}{\lambda} n_0 \int_0^\infty dx \frac{I_i e^{-\alpha_0 x}/I_s}{1+(I_i e^{-\alpha_0 x}/I_s)} = \frac{2\pi}{\lambda}\frac{n_0}{\alpha_0} \ln\left(\frac{1+(I_i/I_s)}{1+(I_i/I_s)\, e^{-\alpha_0 L}}\right). \quad (3)$$

In a similar way the effective change in absorption due to saturation is obtained:

$$\Delta\alpha L = -\ln\left(\frac{1+(I_i/I_s)}{1+(I_i/I_s)\, e^{-\alpha_0 L}}\right). \quad (4)$$

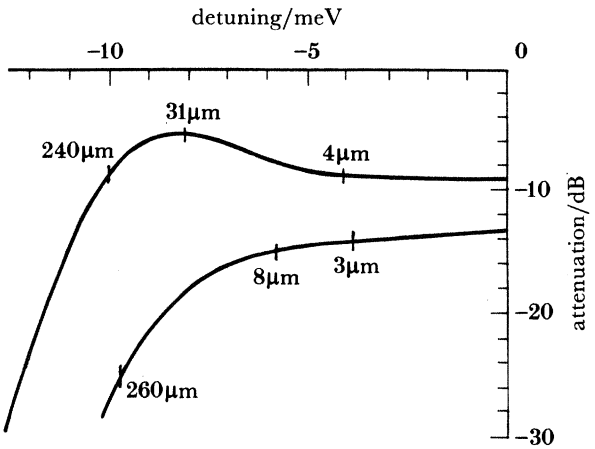

FIGURE 6. Throughput of a waveguide interferometer as a function of detuning from heavy-hole exciton absorption peak. A Gaussian profile for $\alpha_0(\omega)$ has been assumed. Pulse width is 15 ps. Curves are for 1 W (upper) and 0.1 W (lower). Length L of m.q.w. is indicated. A filling factor of 5% is assumed.

Figure 6 shows a plot of the waveguide interferometer throughput in the 'ON' state (symmetry assures a 0 in the 'OFF' state) as a function of frequency detuning from line centre of the heavy-hole exciton. The curves in this graph show the optimum throughput attainable as the frequency is varied, and the input power and pulse length are held fixed. As the detuning is increased, the loss gets lower but the saturation intensity increases in turn. At a detuning of approximately 9 meV, a device 30 μm in length can be operated with 15 ps pulses and about 6 dB throughput loss. Notice that the actual nonlinear interaction length in the waveguide is approximately 20 times greater, because the entire waveguide cross section is not filled with m.q.w. material.

4. SWEEPOUT BY DIFFUSION

If the device is to be speeded up by sweepout, the carriers have to be removed sufficiently rapidly that no carrier buildup occurs in c.w. operation. Suppose each optical pulse produces N_0 carriers. Suppose further that the input digital signal can be represented by the random sequence $f(n)$, where f takes on the values 0 and 1 with equal probability. Each pulse is assumed to produce the number of carriers N_0 needed to produce a π phase shift, and pulses are separated by a time T. Immediately after the $n = 0$ pulse has arrived, the total number of carriers is given by

$$N(nT)|_{n=1} = N_0 f(0) + N_0 \sum_{m=1}^{\infty} f(m)\, a^m, \quad (5)$$

where $a(<1)$ is the fraction of the carriers that remain after time T. If the device works reactively, the average response becomes (neglecting background absorption)

$$\frac{I_0}{I_i} = 1 - \tfrac{1}{8}\pi^2 \frac{a^2}{(1-a^2)\,(1-a)}, \tag{6}$$

where the second term represents a bias due to the long-term accumulation of carriers in the quantum well material. The root mean square deviation of the throughput (σ) is computed similarly and tabulated in table 2. In order to achieve a root-mean-square deviation of less than 5% we need to sweep out at least 80% of the carriers between pulses.

TABLE 2. ROOT-MEAN-SQUARE FLUCTUATIONS ON NORMALIZED OUTPUT INTENSITY

(The variable a is the fraction of carriers remaining in the m.q.w. material after one inter-pulse period.)

a	0.1	0.2	0.3	0.4
σ	0.01	0.06	0.17	0.40

If the carrier sweepout occurs by diffusion, two separate limits can be considered in estimating the device speed. The speed can be underestimated by assuming that diffusion is one-dimensional both inside and outside the quantum well material with the same diffusion constant D (ambipolar). For this case, the number of carriers left inside a layer of width W is given by

$$N(x,t) = N_0\, \mathrm{e}^{-x^2/4Dt'}/\sqrt{(4Dt')}, \tag{7}$$

where $t' = t + W_0^2/2D$ and W_0 is determined from the width of the initial distribution. The number of carriers remaining inside the layer as a function of time is easily expressed in terms of the error function.

Since carrier diffusion outside the layers is essentially two-dimensional and therefore much more rapid, the other limit is obtained by assuming that the carrier distribution vanishes at the layer edges. For this case, the carrier distribution is given by

$$N(x,t) = N_0\, W \tfrac{1}{2}\pi \cos(\pi x/W)\, \mathrm{e}^{-t/\tau}, \tag{8}$$

where $\tau = W^2/(\pi^2 D)$. Notice that the carrier distribution decays much more rapidly in this case owing to the exponential time dependence. If we assume that the curvatures of the carrier distributions are the same at the origin, these two cases are illustrated in table 3. For ambipolar

TABLE 3. FRACTION OF CARRIERS (PERCENTAGES) REMAINING IN THE M.Q.W. MATERIAL AT VARIOUS TIMES

(Case 1 is the Gaussian distribution (equation (7)); case 2 is the cosine distribution (equation (8)). The diffusion constant is 20 $\mathrm{cm^2\ s^{-1}}$.)

time/ps	case 1	case 2
0	100	100
50	45	37
150	28	5
300	20	0.2

diffusion $D \approx 2D_h$ and is taken to be 20 $\mathrm{cm^2\ s^{-1}}$ for this example. Although the actual device recovery time lies somewhere between these two cases, 300 ps should be adequate to sweep out 80% of the carriers.

PHILOSOPHICAL TRANSACTIONS OF THE ROYAL SOCIETY A MATHEMATICAL, PHYSICAL & ENGINEERING SCIENCES

5. Conclusions

We have described an experiment on an all-optical waveguide modulator that showed a response on a picosecond timescale. Full modulation or operation of the device as a logic gate called for an exorbitant peak power in the $LiNbO_3$ realization. A GaAlAs waveguide system would permit operation at greatly reduced, and thus realizable peak powers. To reduce power requirements to levels available from semiconductor laser diodes, greater optical nonlinearities than those available in bulk GaAs are required.

An m.q.w. structure was investigated with this objective, with the natural relaxation time speeded up by carrier diffusion. An optical gate design was carried out that predicts pulse separation times less than 300 ps and peak powers of 1 W with pulse widths of 15 ps. Note that the m.q.w. model gave a net loss. This is characteristic of a two-level system with an appreciable linear loss coefficient α_0 that decreases, roughly, with the square of the frequency deviation from line centre, and a nonlinear index that decreases with the inverse of the cube of the frequency deviation. The detuning cannot decrease the linear loss $e^{-\alpha_0 L}$ sufficiently if a net nonlinear phase shift of π is requred within the length L. A minimum insertion loss is found, as in figure 5. Net loss is also found when the controlled mode is made more intense than the control mode. The throughput is defined as the intensity of the output pulse of the controlled mode divided by the intensity of the input pulse of the control mode.

The set of numbers found in this investigation is not yet as good as one would need for practical all-optical signal-processing devices, but improvement of these numbers by an order of magnitude through the use of a higher optical nonlinearity could make these devices of practical importance. The intensive work on nonlinear optical phenomena currently pursued in several laboratories may arrive at improved materials. We are not aware of any fundamental physical constraints that would prevent such hoped-for improvements.

This work was supported in part by the National Science Foundation under grant no. ECS83-10718.

References

Chemla, D. S., Miller, D. A. B., Smith, P. W., Gossard, A. C. & Weigmann, W. 1984 *IEEE Jl Quantum Electron.* (In the press.)

Chen, Y. J. & Carter, G. M. 1982 *Appl. Phys. Lett.* **41**, 307.

Fujimoto, J. G., Weiner, A. M. & Ippen, E. P. 1984 Submitted to *Appl. Phys. Lett.*

Gibbs, H. M., McCall, S. L., Venkatesan, T. N. C., Gossard, A. C., Passner, A. & Wiegmann, W. 1979 *Appl. Phys. Lett.* **35**, 451.

Kasper, B. L., Link, R. A., Campbell, J. C., Dentai, A. G., Vadhanek, R. S., Henry, P. S., Kaminow, I. P. & Ko, J. S. 1983 In *Digest of the 9th European Conference on Optical Communications, Geneva*, post-deadline paper.

Lattes, A., Haus, H. A., Leonberger, F. J. & Ippen, E. P. 1983 *IEEE Jl Quantum Electron.* **QE-19**, 1718.

PHILOSOPHICAL TRANSACTIONS OF THE ROYAL SOCIETY A MATHEMATICAL, PHYSICAL & ENGINEERING SCIENCES